

# Application of Response Surface Methodology for Catalytic Hydrogenation of Nitrobenzene to Aniline Using Ruthenium Supported Fullerene Nanocatalyst

**Keypour, Hassan\*<sup>+</sup>**

*Faculty of Chemistry, Bu-Ali Sina University, P.O. Box 65175 Hamedan, I.R. IRAN*

**Noroozi, Mohammad**

*Center for Research and Development of Petroleum Technologies at Kermanshah, Research Institute of Petroleum Industry (RIPI), Kermanshah, I.R. IRAN*

**Rashidi, Alimorad**

*Research Institute of Petroleum Industry (RIPI), P.O. Box 14665 Tehran, I.R. IRAN*

**Shariati Rad, Masoud**

*Faculty of Chemistry, Razi University, P.O. Box 6714 Kermanshah, I.R. IRAN*

**ABSTRACT:** *In this study fullerene functionalized using oleum ( $H_2SO_4 \cdot SO_3$ ), followed by the hydrolysis of the intermediate cyclosulfated fullerene as well as an oxidizing agent was employed to functionalize the fullerenes. Ruthenium was then added by the impregnation method or deposited on the functionalized fullerene. Subsequent to this step, Response Surface Methodology (RSM) was used to study the cumulative effect of various parameters including, pressure, temperature, time and loading. In order to maximize the hydrogenation of nitrobenzene (NB) to aniline (AN) these latter parameters were optimized. Furthermore, catalytic activity was evaluated over a temperature range of 25–150°C, hydrogen pressure of 1–30 atm, ruthenium content of 1–15%(w/w) and reaction time of 30–180 min in a bench scale reactor. The optimized model predicted that the hydrogenation should be at a maximum level (approximately 100%) with the following conditions; Ru loading of 15%, reaction temperature of 150 °C, reaction time of 180 min and hydrogen pressure of 22.33 atm.*

**KEY WORDS:** *Hydrogenation, Nitrobenzene, Aniline, Ruthenium, Fullerene, Response surface methodology.*

## INTRODUCTION

Around 85% of aniline is produced via the hydrogenation of nitrobenzene (NB) [1-3], which can be

performed in gas or liquid phase using supported metal catalysts and organic solvents such as alcohols, acetone,

---

\* To whom correspondence should be addressed.

+ E-mail: [haskey1@yahoo.com](mailto:haskey1@yahoo.com)

1021-9986/15/1/21

12/\$/3.20

benzene, ethyl acetate, or aqueous acidic solutions [4,5], electrochemical synthesis and iron based reduction in acidic media [6]. The commercial process of highly exothermic catalytic hydrogenation ( $\Delta H = -544$  kJ/mol at 200°C) of nitrobenzene was performed in both vapor and liquid phases. Generally, nitrobenzene is hydrogenated to aniline with the yield of 99% using fixed-bed or fluidized-bed vapor-phase process. Apparently, the most effective catalysts for gas-phase hydrogenation of nitrobenzene are copper or palladium on activated carbon in combination with other metals (Pb, V, Cr) as modifiers to achieve a higher activity and selectivity [6-10]. Generally, the liquid-phase hydrogenation process is operated at temperature of 90 – 200 °C and pressure of 100 – 600 KPa. Also, the liquid phase reaction may be carried out in slurry or in fluidized-bed reactors [11]. Moreover, the hydrogenation of nitrobenzene was also carried out by DuPont in liquid phase using platinum – palladium catalyst on a carbon support with iron as a modifier [12, 13]. *Chun-Hua Li & Co-workers* also carried out hydrogenation of nitrobenzene with the use of Pt/CNT under mild conditions [14]. The obtained aniline from the hydrogenation of NB was then purified by means of a single-step or multi-step distillation process in which aqueous alkali metal hydroxide solution is added to the raw aniline prior to the distillation process [15]. Catalysis has been considered as one of the various possible applications of fullerenes which generate pathways of research with different directions. These can be categorized in three main groups: (i) the use of C<sub>60</sub> as a catalyst [16-18]; (ii) the use of C<sub>60</sub> as a ligand for homogeneous catalysts [19]; (iii) the use of fullerenes as a support medium for heterogeneous catalysis [20-24]. There have been few investigations in relation to the application of the mentioned materials as catalysts or catalyst supports [25]. In the field of heterogeneous catalysis, numerous carbon materials have been applied to disperse and stabilize nano-sized metallic particles [26]. The Catalytic properties of these solids are known to be dependent on the interaction between the carbon support and metal particles [27, 28]. Solid-state chemistry of fullerene-based materials has gain much interest due to the novel electronic and structural properties of these compounds [29]. In the current paper, the fullerene is used as a support medium for metal catalyst. To investigate the simultaneous influence of pressure, temperature, time and metal loading percentage on the yield of reaction and also determining the best reaction conditions,

Design Of Experiments (DOE) was used. It is notable that the optimization of these parameters required several experiments. Thus, the required numbers of experiments can be reduced by the use of experimental design techniques [30-32]. Central Composite Design (CCD) is an efficient experimental strategy for evaluating the optimum conditions in a multivariable system.

The purpose of the present study is to synthesis fullerene (C<sub>60</sub>)-based ruthenium nanocatalyst that is used for the catalytic hydrogenation of nitrobenzene to aniline. In this study, a new method (involves a combination of impregnation, ultrasound and reduction methods) was used to produce these catalyst and an oxidizing agent was employed to functionalize the fullerenes.

## EXPERIMENTAL SECTION

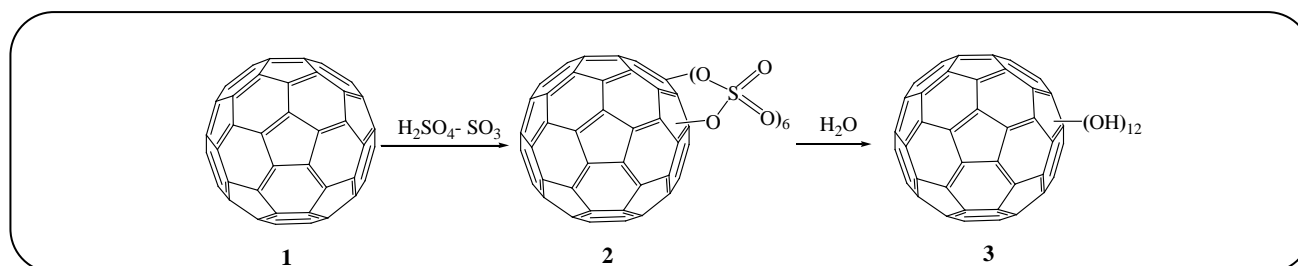
Fullerene (C<sub>60</sub>) was purchased from Sigma-Aldrich Chemise GmbH Company (purity 99%). Solvents and metal salts were purchased from Merck and Alderich, respectively. All materials were employed without further purification. The detection was performed with IR spectra; Shimadzu Fourier Transform Infrared spectra (FT-IR) 8400, FT-NMR Jeol 90 MHz, and SRI8610C Gas Chromatography (GC).

### *Pretreatment of fullerene*

The procedures were briefly summarized as follows: A reaction flask (50 mL) charged with 1.0 g fullerene and fuming sulfuric acid (15 mL) was stirred at 55 – 60 °C under N<sub>2</sub> for 3 days to give a dark brown solution with orange suspensions. The resulting mixture was added dropwise into anhydrous diethyl ether (200 mL) with vigorous stirring in an ice bath to cause the precipitation of products. Precipitates were separated from solution by the centrifuge technique. They were then washed and centrifuged three times with anhydrous diethyl ether and twice with 2:1 anhydrous diethyl ether-acetonitrile and dried in vacuum at 40 °C to afford a brown-orange solid of polycyclosulfated fullerene derivative 2 (1.3 g). A reaction flask (100 mL) equipped with a condenser and an inert gas bubbler was charged with polycyclosulfated fullerene derivative 2 (1.0 g) and distilled water (20 mL). The mixture was stirred at 85 °C under N<sub>2</sub> for 10 h to give a dark brown suspension. The suspended solid was separated from aqueous solution by centrifugation followed by washing twice with water and drying in vacuum at 40 °C to afford a brown solid of polyhydroxylated fullerene derivative 3 (fullerenol)[33].

**Table 1: Dispersion values of the Ru supported on fullerene (C<sub>60</sub>).**

Catalysts	Raw material for metal	Volume of metal salt solution (mL)	Metal loading (w/w %)		Loading efficiency (%)
			Calculated	Found <sup>a</sup>	
Ru-1	RuCl <sub>3</sub> .3H <sub>2</sub> O (4.95 × 10 <sup>-3</sup> M)	10	1	0.92	92.0
Ru-8		80	8	7.49	93.6
Ru-15		150	15	14.75	98.3
<sup>a</sup> As determined by AAS for catalyst					

**Scheme 1: preparation of fulleranol.**

### Preparation of catalysts

Pre-treated fullerene (0.5 g) were first mixed with 10, 80 or 150 ml of aqueous solution of the metal salt RuCl<sub>3</sub>.3H<sub>2</sub>O (4.95 × 10<sup>-3</sup>M), to obtain catalysts containing 1, 8 or 15% Ru/C<sub>60</sub>, respectively (Table 1). In order to enhance penetration and dispersion of metal into the catalyst, citric acid (0.015 mol) was added to each solution [34, 35]. By adding appropriate amount of ethanol-water (1:3 ratio), the final volume will be increased up to 200 mL. Each suspension was completely mixed at 50°C in the periodic 6 h with vigorous stirring and then sonicated to form a uniform suspension for 30 min in ultrasonic bath (1.6 MHz). Subsequently, it was cooled in a cold water bath, filtered and finally washed with a large amount of ethanol and deionized water. Elemental analysis was applied to determine the trace of metal species, indicated the fact that all metal particles were adsorbed on the support surface completely. In order to remove the solvent, the resulting slurry was dried at 100 °C, and then was calcinated in air at 550°C for 4 h. As a result, the obtained samples were reduced with pure H<sub>2</sub> (400 ml/min) at 300°C and atmospheric pressure for 3 h. Finally, the percentage of metal loading in the catalysts was measured by atomic absorption spectrophotometer (AAS) (Table 1).

### Catalyst characterization

The Transition Electron Microscopy (TEM) images were taken on a Philips CM120 at an accelerating voltage

of 120Kv. Thermogravimetric analysis (TGA) of the dried samples was performed on a Mettler Toledo TGA SDTA 851e at the temperature range of 30 - 800 °C and the rate of 10 °C/min. X-Ray powder Diffraction (XRD) analysis was conducted by Philips instrument with graphite monochromatic Cu K $\alpha$  radiation ( $\lambda = 1.5418 \text{ \AA}$ ) to confirm the formation of products.

The quantitative determination of active catalyst was carried out by a SHIMADZU AA-6100 atomic absorption spectrometer by dissolving the samples in a mixture of HCl and HNO<sub>3</sub> with the 3:1 ratio at 40°C for 24 h. Gas chromatography (GC) was carried out by SRI with a Flame Ionization Detector (FID) and the following conditions: injector 250 °C, FID, 250 °C, column MXT -624 (6% Cyanopropyl phenyl, 94% dimethyl polysiloxane, 30 meter, 0.53 mm ID) and column temperature program 100 to 215°C with the rate of 5°C/min, Carrier gas: helium, sample size: 0.1  $\mu$ L and total cycle time, 23 min.

### Catalytic test

#### Reactor reaction

0.1 g the of synthesized catalyst Ru/C<sub>60</sub> was introduced into a 100 mL stainless steel autoclave reactor and reduced under the flow of H<sub>2</sub> at 300 °C for 1 h. Then 2 mL of nitrobenzene (extra pure) and 10 ml of toluene (Merck, extra pure), was added to the reactor as a solvent. In the aim of removing any oxygen, the mixture

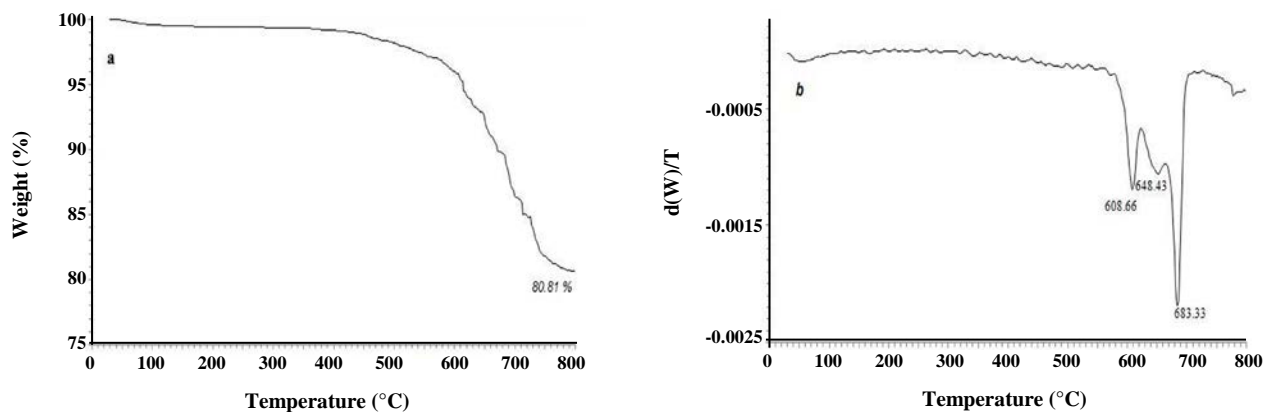


Fig. 1: (a) TGA and (b)  $d(W)/T$  profiles of Ru catalyst.

was purified with  $N_2$  for 10 min. The reaction was carried out in different conditions; hydrogen pressure (1-30 bar), temperature (25-150 °C), and duration (30-180 min). The yield of hydrogenation was then determined by GC.

*Central composite design analysis and optimization of the response surface methodology associated with the hydrogenation of nitrobenzene*

The effect of various parameters, including, initial pressure of hydrogen (P), temperature (T), reaction time and the amount of loading (L) of ruthenium in the catalyst on the hydrogenation efficiency of NB to AN was studied by statistically designed experiments and optimized by response surface methodology. A central composite design with  $\alpha = 1$  and one replicate at the center point, resulting in experiments for each catalyst which covers the entire range of variables, were used to optimize the chosen key variables for the hydrogenation of NB using batch reactor.

The design package Minitab 14 is a statistical program package that was used for the regression analysis of the obtained data. Moreover, this design evaluates the coefficient of the regression equation. The equation was confirmed by the analysis of variance (ANOVA) to determine the significance fitness of each term in the equations and to estimate goodness of fit in each case. Conditions of the hydrogenation were as follows; pressure, temperature, time, and catalyst metal loading. In the current study, these conditions were varied from 1 to 30 atm, 25 to 150 °C, 30 to 180 min, and 1 to 15 % respectively. Low, middle and high levels of each variable were determined as 1, 0 and +1, respectively. Coded and actual values of four independent variables of

Ru along with the response for Response Surface Methodology (RSM) are shown in Table 2

## RESULTS AND DISCUSSION

### *Thermogravimetric analysis*

The thermal analysis data in inert atmosphere ( $N_2$ ) are shown in Fig. 1. This curve is related to ruthenium catalyst with 15% loading. Two main weight loss regions were observed in this figure. The first weight loss occurred at a temperature range of 100°C - 650°C and was moderate. Another weight loss was observed the temperature range of 660°C -750°C. Results show that solvent losses such as water and organic solvents in catalyst starting at 100°C and carbon cage and amorphous carbon decomposing at 650°C [34]. The remaining weight percent up to the temperature of 800 °C is equal to 80.81. High level of residual mass may be due to the presence of metal installed on the fullerene, perform TGA under nitrogen atmosphere and the calcined in air at 550 °C for 4 h.

### *X-ray Diffraction analysis*

The crystalline structure of the catalyst was obtained using powder XRD. The typical XRD pattern of Ru/C<sub>60</sub> is presented in Fig. 2. The assignment of the various crystalline phase was based on the JPDS powder diffraction file card [37]. The particle size of each phase was calculated from the line broadening of the most intense reflections using the Scherrer equation. Estimated errors of the particle sizes and relative percentage of different phase is about of 10% [38-41].

The XRD pattern obtained for the Ru/C<sub>60</sub> showed lower crystallinity. The peaks at a  $2\theta$ : 38.6, 42.3, 44 and 58.3

**Table 2: Central composite design matrix, levels of the variables, observed and predicted responses for the hydrogenation of nitrobenzene to aniline by Ru catalyst.**

Run no.	Pressure (atm)	Temperature (°C)	Time (min)	Loading (%)	hydrogenation efficiency %		
					Found <sup>a</sup>	Predicted	Residual
					-0.2348		
1	30.0	25.0	30	15	73	73.2348	
2	15.5	87.5	105	8	65	70.8480	-5.8480
3	30.0	150.0	180	1	90	81.6792	8.3208
4	30.0	25.0	180	1	67	71.2903	-4.2903
5	15.5	87.5	30	8	61	60.7884	0.2116
6	30.0	150.0	30	15	93	86.6237	6.3763
7	15.5	87.5	105	8	68	70.8480	-2.8480
8	15.5	150.0	105	8	69	81.1218	-12.1218
9	15.5	87.5	105	8	65	70.8480	-5.8480
10	1.0	150.0	180	15	82	80.5681	1.4319
11	30.0	25.0	30	1	56	55.0126	0.9874
12	30.0	150.0	30	1	58	63.4014	-5.4014
13	15.5	87.5	180	8	74	73.5662	0.4338
14	1.0	25.0	30	1	38	39.1792	-1.1792
15	15.5	87.5	105	8	68	70.8480	-2.8480
16	1.0	150.0	30	1	45	41.5681	3.4319
17	15.5	87.5	105	1	67	62.5662	4.4338
18	1.0	25.0	30	15	58	63.9014	-5.9014
19	30.0	25.0	180	15	83	84.0126	-1.0126
20	1.0	150.0	180	1	54	56.3459	-2.3459
21	1.0	87.5	105	8	59	55.0107	3.9893
22	30.0	87.5	105	8	69	72.3440	-3.3440
23	30.0	150.0	180	15	98	99.4014	-1.4014
24	1.0	25.0	180	15	74	71.1792	2.8208
25	15.5	25.0	105	8	85	72.2329	12.7671
26	1.0	150.0	30	15	73	71.2903	1.7097
27	15.5	87.5	105	8	76	70.8480	5.1520
28	15.5	87.5	105	8	76	70.8480	5.1520
29	1.0	25.0	180	1	48	51.9570	-3.9570
30	15.5	87.5	105	8	76	70.8480	5.1520
31	15.5	87.5	105	15	80	83.7884	-3.7884
Factors		Levels					
				-1	0		1
Pressure (atm)				1.0	15.5		30.0
Temperature (°C)				25.0	87.5		150.0
Time (min)				30	105		180
Loading (%)				1.0	8.0		15.0

which agree well with the known diffraction pattern of ruthenium (JCPDS 6-663). The obtained cluster size of ruthenium nanoparticles using the Scherrer formula is 20.3 nm.

### Transmission Electron Microscopy (TEM)

The estimation of the average ruthenium particle size was carried out by TEM for catalyst. Average metal particle size of Ru was 15.7 nm. The particle size of large metals in the former catalyst were determined by TEM and XRD data. Fig. 3 shows the TEM image of a catalyst. As observed in this figure, most of the ruthenium particles were located on the external surface of the fullerene.

### FT-IR spectroscopy

The FT-IR spectra of the solvent, reactant and product are shown in Fig. 4. A mixture of reactants containing toluene and NB are shown in Fig. 4a. Fig. 4b illustrates that the new peaks at 3100-3500  $\text{cm}^{-1}$  are associated to the N-H stretching region. Two bands were appeared at 3400 and 3300  $\text{cm}^{-1}$  indicating the fact that the product is a primary amine. The High frequency band is related to the asymmetric vibration, While, the low frequency band is related to the symmetric vibration. The low intensity shoulder is due to the N-H asymmetric vibration band which appears at 3200  $\text{cm}^{-1}$ , and the symmetric vibration appears around 1600  $\text{cm}^{-1}$ . A broad (medium to strong intensity) peak appeared in 1640-1560  $\text{cm}^{-1}$ , which belongs to the N-H bending mode. An out of plane N-H bending vibration appears as a broad band at 800  $\text{cm}^{-1}$ . The C-N stretching absorption emerges within the range of 1350-1250  $\text{cm}^{-1}$  [42].

### Efficiency of hydrogenation

1  $\mu\text{L}$  of pure nitrobenzene, aniline and toluene were injected separately into the GC column and the spectra of each samples show a peak with clear retention time. Then 1  $\mu\text{L}$  of the mixture was injected to the reactor and the obtained spectra compared with the spectra of pure nitrobenzene, aniline and toluene. By dividing the area under the peak of aniline (Aa) to the total area of aniline and nitrobenzene peaks (At), and multiply the resulting number to 100 (Eq.1)

The hydrogenation efficiency can be calculated by the following method. First, at the set-up process, various

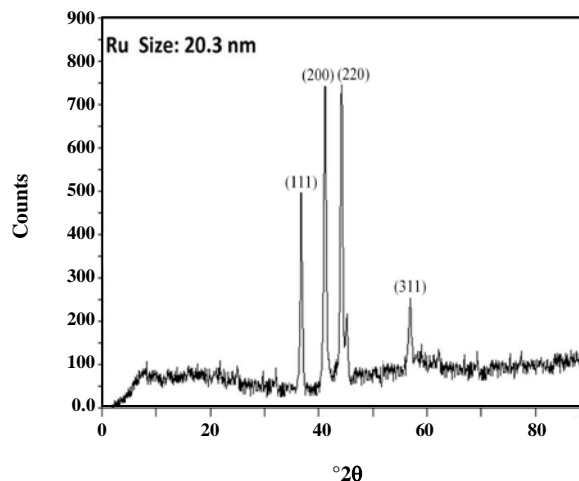


Fig. 2: XRD pattern of nano catalyst Ru/C<sub>60</sub>.

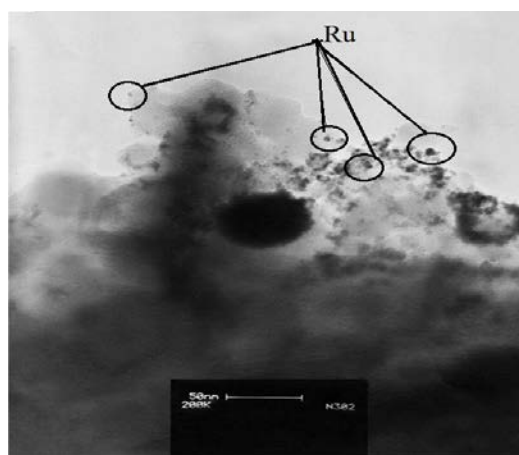


Fig. 3: TEM micrographs of the Ru.

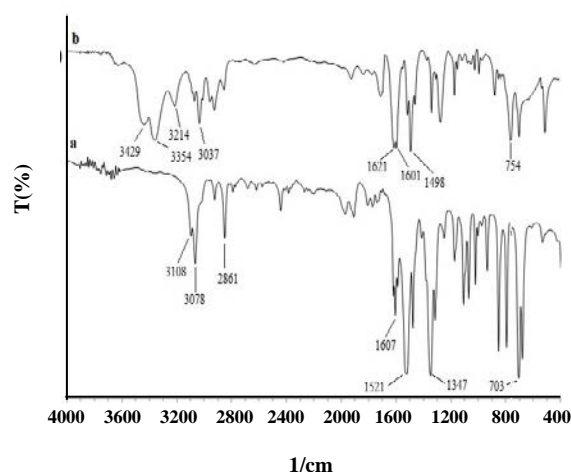


Fig. 4: FT-IR spectrum (a) nitrobenzene (b) aniline.

**Table 3: Analysis of Variance for Efficiency (%).**

Source	DF <sup>a</sup>	Seq SS <sup>b</sup>	Adj SS <sup>c</sup>	Adj MS <sup>d</sup>	F <sup>e</sup>	P <sup>f</sup>
Regression	14	4867.3	4867.3	347.66	7.14	0.000
Linear	4	4469.0	565.5	141.37	2.90	0.055
Square	4	248.5	248.5	62.13	1.28	0.320
Interaction	6	149.7	149.8	24.96	0.51	0.790
Residual Error	16	779.1	779.1	48.69		
Lack-of-Fit	10	615.4	615.4	61.54	2.26	0.166
Pure Error	6	163.7	163.7	27.29		
Total	30	5646.4				

a) Degree of freedom.

b) Sequential sum of squares.

c) Adjusted sum of squares.

d) Adjusted mean of squares.

e) F test.

f) p value.

parameters such as temperature of column, injector and detector were adjusted. Then, hydrogenation product (1 $\mu$ L) injected into the GC column. Aniline was the only product of the nitrobenzene hydrogenation that is detected by GC chromatography. The efficiency of aniline is obtained from the following formula:

$$\text{Efficiency(\%)} = \frac{A_a}{A_t} \times 100 \quad (1)$$

Where 'Aa' is the area under the aniline peak, 'At' is the area under the aniline and nitrobenzene peaks in the mixture of the reactor. The determined efficiencies by CG chromatography are shown in table 2.

#### **Analysis of variance (ANOVA) and estimated regression coefficient for the response Y**

A series of experiments were carried out by considering a central composite design (Table 2). Various statistical data (standard error of estimate, sum of squares of the errors, F statistics and p value) were also calculated. The collected statistical data in Table 3 indicate that the model containing linear, squared and interaction terms is significant at 95% confidence level ( $p=0$  and  $F=7.14$ ). This means that the model is reliable and can be used in the prediction purposes. Moreover, among different sources of variation in the model, the linear part is significant at 90% confidence level ( $p < 0.1$ ). The coefficients of the nonlinear polynomial model and p values are shown in Table 4, where the standard error of coefficient is a measure of the variation in estimating the coefficient and "t" is the ratio of the coefficient to the standard error. At 95% confidence level, only pressure

and constant terms are significant ( $p < 0.05$ ). The sign of the pressure term indicates that in higher hydrogen pressures, the efficiency of the hydrogenation will be higher. Moreover, the coefficients of the squared and interaction terms were relatively small.

#### **Model validation**

Experimental results, predicted values, and the coefficients in Table 4, were used to calculate the residuals. Fig. 5 shows the normal probability of the residuals distribution. The correlation between the observed and predicted values of efficiency in hydrogenation is relatively acceptable (with coefficient of determination equal to 86.2%).

#### **Response surface plots**

In order to gain an insight about the effect of each variable, three dimensional (3D) plots for the predicted responses were also obtained. These curves have been plotted based on the polynomial function model with the use of the coefficients in Table 4 to illustrate changes in the response surface (Fig. 6). In these curves, there is a significant relationship between variables and response (efficiency %) at the center level of other variables. For example, Fig. 6a shows the effect of Ru loading (L) and reaction time (Time) on the efficiency of the hydrogenation of the NB (E (%)) at the center level of reaction temperature (T) and hydrogen pressure (P). The effect of reaction temperature (T) and Ru loading (L) on efficiency (E (%)), while keeping reaction time (Time) and hydrogen pressure (P) at center level, was shown in Fig. 6b.

**Table 4: Estimated Regression Coefficients for Efficiency (%).**

Term	<sup>a</sup> Coef	<sup>c</sup> T	<sup>d</sup> P
Constant	35.718	3.852	0.001
Pressure	1.5537	2.205	0.042
Temperature	-0.2498	-1.222	0.239
Time	0.2214	1.300	0.212
Loading	1.0284	0.668	0.514
Pressure*Pressure	-0.0341	-1.655	0.117
Temperature*Temperature	0.0015	1.346	0.197
Time*Time	-0.0007	-0.847	0.409
Loading*Loading	0.0475	0.538	0.598
Pressure*Temperature	0.0017	0.860	0.403
Pressure*Time	0.0008	0.502	0.623
Pressure*Loading	-0.0160	-0.931	0.365
Temperature*Time	0.0001	0.287	0.778
Temperature*Loading	0.0029	0.717	0.484
Time*Loading	-0.0026	-0.788	0.442

a) Coefficient. b) Standard error of the coefficient. c) t test. d) p value

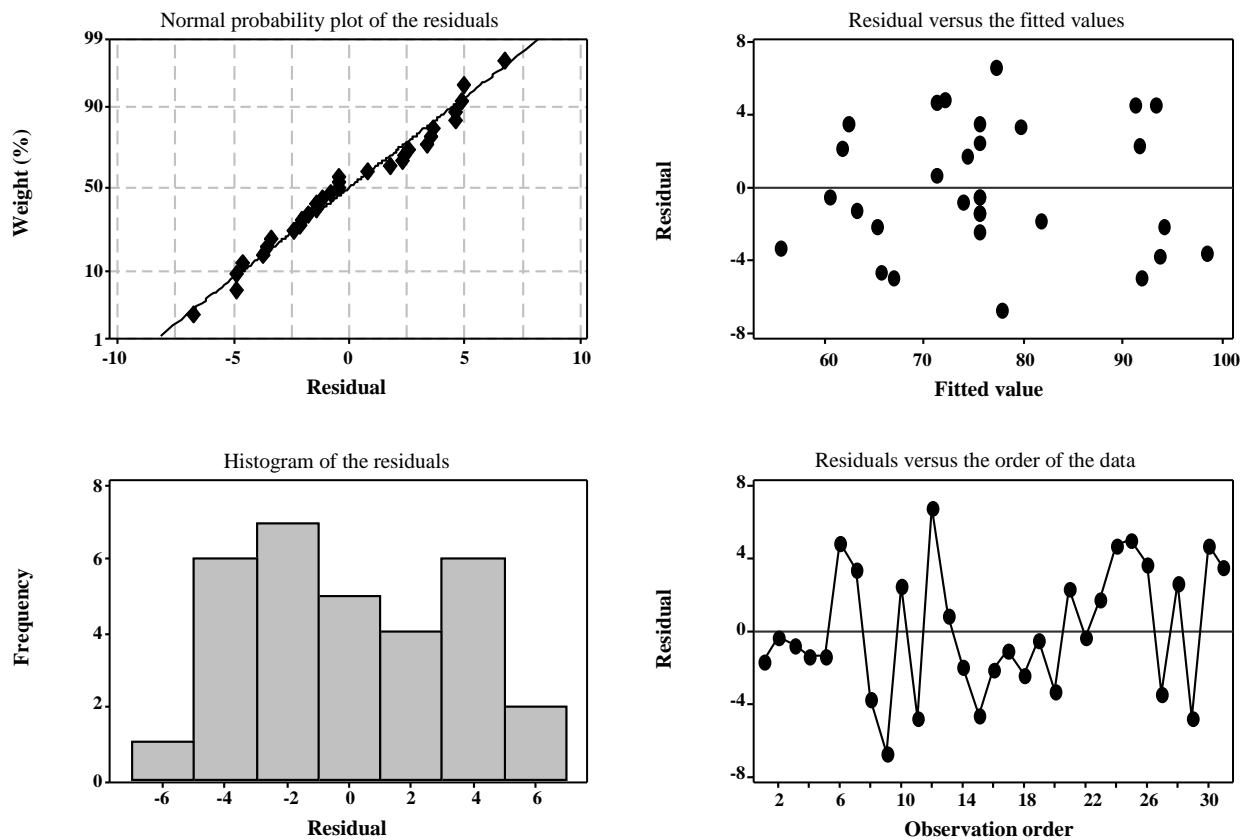
**Residual plots for Efficiency (%)****Fig. 5: Residual plots for Y (efficiency (%)) in the model.**



Table 5: Optimum values of variables obtained from regression equations for the hydrogenation of nitrobenzene to aniline

Parameter	Pressure (atm)	Temperature (°C)	Time (min)	Loading (%)	Hydrogenation (%)
Optimum value	22.33	150.00	180.00	15.00	100.00

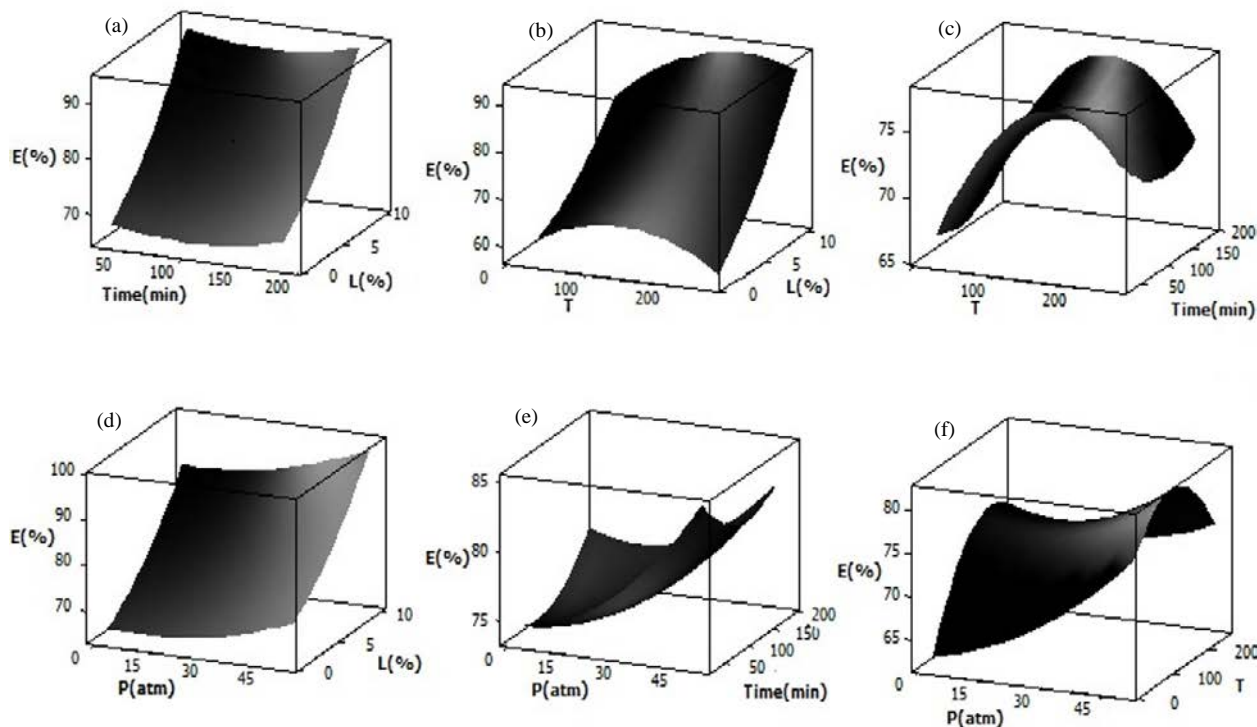


Fig. 6: The three-dimensional (3D) plots of efficiency of hydrogenation of NB.

Surface plots of the efficiency (%) versus pressure and loading, pressure and time, temperature and time, and pressure and temperature were also shown in Figs. 6c, 6d, 6e and 6f, respectively. As shown in Figs. 6a, b, c, d, e, f, there is a nonlinear relationship between E (%) and P, T, Time and L variables, since there are a few curves were observed at the surface plots of E (%). Response optimization results of the nonlinear polynomial model are shown in Table 5. The optimal values of the variables are also reported in Table 5 and can be simply observed in the different panels in Fig. 6.

Multiple regression analysis of the experimental data was obtained from the following regression equation for the hydrogenation of benzene: in which Y is the response variable or hydrogenation efficiency of benzene P, T, t and W are the coded values of the independent variables, pressure, temperature, reaction time and metal loading percentage, respectively.

$$Y = 35.718 + 1.5537P - 0.2498T + 0.2214t + 1.0284W - 0.0341P^2 + 0.0015T^2 - 0.0007t^2 - 0.0475W^2 + 0.0017PT + 0.0008Pt - 0.0160PW + 0.0001Tt + 0.0029TW - 0.0026tW \quad (2)$$

The multiple regression coefficient ( $R^2$ ) was estimated from the second-degree polynomial Eq. (2). The value of  $R^2 = 0.924$ , which is close to one, indicates that the correlation is suitable for predicting the performance of the hydrogenation system and the predicted values were close to the experimental results.

Metals have different physical and chemical properties. So they have different catalytic activities. Since ruthenium catalysts were shown to be highly active and selective for the hydrogenation of aromatic amines [43]. Usefulness of ruthenium as hydrogenation catalysts has been recognized by many other investigators in various hydrogenations [44, 45].

However, what is clearly seen in this study is that the use of fullerene as a base in the preparation of catalysts increased the efficiency of hydrogenation. It will definitely increase the active surface of the catalyst.

## CONCLUSIONS

In this study ruthenium nanocatalyst supported fullerenes (C<sub>60</sub>), used for the catalytic hydrogenation of NB to AN, was investigated. This catalyst was characterized by different instrumental techniques and the activity of the hydrogenation of NB to AN in a batch reactor was also tested. Subsequent to this step, response surface methodology (RSM) was used to study the cumulative effect of various parameters including, pressure, temperature, time and loading. In order to maximize the hydrogenation of NB to AN these latter parameters were optimized. Furthermore, catalytic activity was evaluated over a temperature range of 25–150°C, hydrogen pressure of 1–30 atm, ruthenium content of 1–15% (w/w) and reaction time of 30–180 min in a bench scale reactor. The optimized model predicted that the hydrogenation should be at a maximum level (approximately 100%) with the following conditions; Ru loading of 15%, reaction temperature of 150 °C, reaction time of 180 min and hydrogen pressure of 22.33 atm.

## Acknowledgments

We are grateful to the Department of Chemistry of Bu-Ali Sina University and Center for Research and Development of Petroleum Technologies at Kermanshah, Research Institute of Petroleum Industry (RIPI), Kermanshah, Iran, for financial support.

Received : Jul. 17, 2013 ; Accepted : Oct. 27, 2014

## REFERENCES

- [1] Rode C.V., Vaidya M.J., Jaganathan R., Chaudhari R.V., [Hydrogenation of Nitrobenzene to p-Aminophenol in a Four-Phase Reactor: Reaction Kinetics and Mass Transfer Effects](#), *Chem. Eng. Sci.*, **56**:1299-1304 (2001).
- [2] Lee L.T., Chen M.H., Yao C.N., [Process for Manufacturing p-Aminophenol](#), *US patent 4, 885,389* (1998).
- [3] Chaudari R.V., Divekar S.S., Vaidya M.J., Rode C.V., [Single Step Process for the Preparation of p-Aminophenol](#), *US patent 6,028,227* (2000).
- [4] Figueras F., Coq B., [Hydrogenation and Hydrogenolysis of Nitro-, Nitroso-, Azo-, Azoxy- and Other Nitrogen-Containing Compounds on Palladium](#), *J. Mol. Catal. A Chem.*, **173**:223-230 (2001).
- [5] Torres C., Jablonski C., Baronetti E.L., Castro G.T., de Miguel S.R., Scelza O. A., et al., [Effect of the Carbon Pre-treatment on the Properties and Performance for Nitrobenzene Hydrogenation of Pt/C Catalysts](#), *J. Appl. Catal. Gen.*, **161**: 213-226 (1997).
- [6] Yun K. S., Cho B. W., [Process for Preparing Para-Aminophenol](#), *US patent 5, 066, 369* (1991).
- [7] Lonza. First Chemical Co, *Hydrocarbon Process*, **59**:136-143 (1979).
- [8] Szigeth L., [Method for the Catalytic Hydrogenation of Organic Nitro Derivatives in the Gaseous State to Corresponding Amines](#), *US patent 3,636,152* (1972).
- [9] Jurden Z., [Process for the Catalytic Hydrogenation of Nitrobenzene](#), *EP 011090* (1979).
- [10] Adams E.G., Barker R.B., Lossett M.J., Flowers L.I., [Co-Production of an Aromatic Monoamine and an Aromatic Diamine Directly from Benzene or a Benzene Derivative Through Controlled Nitration](#), *US Patent 4,740,621* (1986).
- [11] Cooke E.V., Thurlow H.J., [Catalytic Hydrogenation of Nitro Aromatic Compounds to Produce the Corresponding Amino Compounds](#), *US Patent 3,270,057* (1964).
- [12] Gonzalez R.A., [Hydrogenation F Aromatic Nitro Compounds](#), *US Patent 3,499,034* (1966).
- [13] Cossaboon K.F., [Hydrogenation of Mixed Aromatic Nitro bodies](#), *US Patent 4,185, 036* (1977).
- [14] Li C.H., Yu Z.X., Yao K.F., Ji S.F., Liang J., [Nitrobenzene Hydrogenation with Carbon Nanotube-Supported Platinum Catalyst Under Mild Conditions](#), *Journal of Molecular Catalysis A. Chemical .*, **226**: 101-105 (2005).
- [15] Markus D., Gehlen V., Wershofen F. U., Andre L., Peter L., Benie W.M., [Process for Preparing Aniline](#), *US 7692042* (2010).
- [16] Panagiotou G.D., Tzirakis M.D., Vakros J., Loukatzikou L., Orfanopoulos M., Kordulis C., et al., [Development of \[60\] Fullerene Supported on Silica Catalysts for the Photo-Oxidation of Alkenes](#), *Appl.Catal.A.*, **372**:16-25 (2010).

- [17] Hino T., Anzai T., Kuramoto N., [Visible-Light Induced Solvent-Free Photooxygenations of Organic Substrates by Using \[60\] Fullerene-Linked Silica Gels as Heterogeneous Catalysts and as Solid-Phase Reaction Fields](#), *Tetrahedron Lett.*, **47**: 1429-1432 (2006).
- [18] Tzirakis M.D., Vakrosb J., Loukatzikouc L., Amargianitakisa V., Orfanopoulousa M., Kordulisb C., Lycourghiotis A.,  [\$\gamma\$ -Alumina-Supported \[60\]Fullerene Catalysts: Synthesis, Properties and Applications in the Photooxidation of Alkenes](#), *J.Mol.Catal. A.*, **316**: 65-74 (2010).
- [19] Sulman E., Matveeva V., Semagina N., Yanov I., Bashilov V., Sokolov V., [Catalytic Hydrogenation of Acetylenic Alcohols Using palladium Complex of Fullerene C<sub>60</sub>](#), *J. Molecular Catal A: Chemical.*, **146**: 257-263 (1999).
- [20] Coqa B., Planeixb J.M., Brotos V.A., [Fullerene-Based Materials as New Support Media in Heterogeneous Catalysis by Metals](#), *Appl. Catal. A.*, **173**: 175-183 (1998).
- [21] Spassova I., Khristova M., Nickolov R., Mehandjiev D., [Novel Application of Depleted Fullerene Soot \(DFS\) as Support of Catalysts for Low-Temperature Reduction of NO with CO](#), *J. Colloid Interface Sci.*, **320**: 186-193 (2008).
- [22] Bai Z., Shi M., Niu L., Li Z., Jiang L., Yang L., [Facile Preparation of Pt-Ru Nanoparticles Supported on Polyaniline Modified Fullerene \[60\] for Methanol Oxidation](#), *Journal Supported on Nanoparticle Research*, **15**: 11-17 (2013).
- [23] Wei G., Wang L. H., Lin Y. J., Yi J., Chen H.B., Liao D. W., [Novel Ruthenium Catalyst \(K-Ru/C60/70\) for Ammonia Synthesis](#), *Chinese Chemical Letters*, **10**: 433-438 (1999).
- [24] Manjon F., Santana M. M., Garcia F. D., Orellana, Guillermo [Are Silicone-Supported \[C60\]-Fullerenes an Alternative to Ru\(ii\) Polypyridyls for Photodynamic Solar Water Disinfection](#), *Photochemical and Photobiological Sciences*, **13**, 397-406 (2014).
- [25] Pol S.V., Pol V.G., Frydman A., Churilov G.N., Gedanken A., [Fabrication and Magnetic Properties of Ni Nanospheres Encapsulated in a Fullerene-like Carbon](#), *J. Phys. Chem. B.*, **109**: 9495-9498 (2005).
- [26] Rylander P.N., "Catalytic Hydrogenation in Organic Synthesis", *Academic Press*, New York, London (1979).
- [27] Trépanier M., Tavasoli. A., Anahid. Sanaz., Dalai. A., [Deactivation Behavior of Carbon Nanotubes Supported Cobalt Catalysts in Fischer-Tropsch Synthesis](#), *Iran. J. Chem. Chem. Eng. (IJCCE)*, **30**:37-47 (2011).
- [28] Tavasoli A., Irani M., Nakhaeipour A., Mortazavi Y., Khodadadi A. A., Ajay K. D., [Preparation of a Novel Super Active Fischer-Tropsch Cobalt Catalyst Supported on Carbon Nanotubes](#), *Iran. J. Chem. Chem. Eng. (IJCCE)*, **28**: 37-48 (2009).
- [29] Fischer J.E., Heiney P.A., Smith A.B., [Solid State Chemistry of Fullerene-Based Materials](#), *Acc. Chem. Res.*, **25**: 112-118 (1992).
- [30] Montgomery D.C., "Design and Analysis of Experiments", John Wiley Publishing Co. (1991).
- [31] Cestari A.R., Vieira E.F.S., Nascimento A.J.P., Santos Filha M.M., Airoidi C., [Factorial Design Evaluation of Some Experimental Factors for Phenols Oxidation using Crude Extracts from Jackfruit \(\*Artocarpus integrifolia\*\)](#), *J. Braz. Chem. Soc.*, **13**: 260-265 (2002).
- [32] Kincl M., Turk, S., Vrecer F., [Application of Experimental Design Methodology in Development and Optimization of Drug Release Methodist](#). *J. Pharm.*, **291**: 39-49 (2005).
- [33] Chiang L.Y., Wang L.Y., Swirczewski J. W., Soled, S., Cameron, S., [Efficient Synthesis of Polyhydroxylated Fullerene Derivatives via Hydrolysis of Polycyclosulfated Precursors.](#), *J. Org. Chem.* **59**: 3960-3968 (1994).
- [34] boule- Gheit A.K. A., [The Role of Additives in the Impregnation of Platinum and Ruthenium on Alumina Catalysts](#), *J. Chem. Tech. Biotechnol.* **29**: 480-486 (1979).
- [35] About- Gheit A.K., "Aromatic Hydrogenation on Supported Bimetallic Combination", Inst. Francais du Petrole. Rep. No., 20874 (1973).
- [36] Saxby J.D., Chatfield S.P., [Thermogravimetric analysis of Buckminsterfullerene and Related Materials in Air](#), *J. Phys. Chem.*, **96**:17-18 (1992).
- [37] "JCPDS Powder Diffraction File", International Centre for Diffraction Data, Swarthmore.

- [38] Nath, S., Chakdar, D., Gope G. [Synthesis of CdS and ZnS Quantum Dots and Their Applications in Electronics](#), *Nanotrends., A Journal of Nanotechnology and its Application.*, **2**:1-3 (2007).
- [39] Nath S., Chakdar, D., Avasthi D., [Novel Effect of 100 MeV Ni<sup>+</sup> 7 Ion Beam on ZnS Quantum dots Prepared by Chemical Methods](#), *Journal of Nanoelectronics and Optoelectronics.*, **3**:1-4 (2006).
- [40] Das R., Nath S.S., Chakdar D., Gope G., Bhattacharjee R., [Preparation of Silver Nanoparticles and Their Characterization Printable Document](#), *Journal of Nanotechnology Online.*, **8**: 4-6 (2008).
- [41] Hall B.D., Zanchet D., Ugarte D., [Estimating Nanoparticle Size from Diffraction Measurements](#), *Journal of Applied Crystallography*, **33**: 1335-1341 (2000).
- [42] Pavia, D. L., Lampman G. M., Kriz G.S., Vyvyan J.R., "Introduction to Spectroscopy", **4**: 76-91 (2009).
- [43] Behr L.C., Kirby J.E., MacDonald R.N., Todd C.W., [Synthesis of Alicyclic Diamines](#), *J. Am. Chem. Soc.*, **68**, 1296-1297 (1946).
- [44] Whitman G. M., [Ruthenium Catalyzed Hydrogenation Process for Obtaining Aminocyclohexyl Compounds](#), *US Patent*. 2,606,925. (1952).
- [45] Nishimura S., Itaya T., Shiota M., [Reactions of Cycloalkanones in the Presence of Platinum-Metal Catalysts and Hydrogen](#), *Chem. Commun. (London)*, 422-423 (1967).